geoconvention
Calgary • Canada • May 12-14 2025

Transitional in-situ stress regime and hydraulic fracturing induced seismicity in the Montney formation

Hongxue Han and Mirko van der Baan
Department of Physics, University of Alberta

Summary

In this study, we investigate slip potentials of variously oriented major faults in the North Montney Trend (NMT) and the Kiskatinaw Seismic Monitoring and Mitigation Area (KSMMA) in the Western Canada Sedimentary Basin (WCSB). The largest recorded M_W=4.6 event occurred on August 17, 2015, in the NMT, and another three events (M_L=3.6~4.3) occurred on November 30, 2018, near the southern margin of the Fort St. John Graben (FSJG) in KSMMA (Table 1).

Table 1 List of focal mechanisms for felt earthquakes in the Montney Formation (magnitude >3.5)

Date	Time	Latitude	Longitude	Magnitude	Strike	Dip	Rake	Reference
2015-08-17		57.01	-122.15	M_W 4.55	323.41	42.01	86.74	Mahani et al., 2017
2018-11-30	2:06:02	56.049	-120.716	M_L 3.62	131.03	61.44	111.41	Salvage and Eaton, 2022
2018-11-30	2:15:00	56.054	-120.691	M_L 4.32	277.14	67.14	-121.89	Salvage and Eaton, 2022
2018-11-30	1:27:06	56.02	-120.52	M_W 4.31	276.46	46.31	60.11	Hamidbeygi et al., 2023

The likelihood of induced seismicity is typically associated with treatments of overpressured reservoirs (Eaton and Schulz, 2018). This study emphasizes the importance of estimating the full stress tensor, for areas close to transtensional or transpressional regimes, as in these cases fault reactivation can occur on multiple planes, typically including both strike-slip and normal, or strike-slip and reverse faults, as well as bedding plane slip.

Method

We first estimate full in-situ stresses for the Montney Formation for the key wells. Magnitude estimation of the maximum horizontal stress is subject to a large uncertainty. We therefore estimate a range of probable values based on the poroelastic stress model, combined with strain corrections inversely proportional to the distance from the Rocky Mountain Fold and Thrust Belt (FTB), as well as commonly used constraints from the borehole measurements and the possibility of a critical stress state (Han and van der Baan, 2024).

Next, we use areal pore pressure, elastic properties, horizontal strain corrections, and vertical stress magnitude (integrated from density logs) maps to estimate the horizontal in-situ stress maps for the Montney Formation including uncertainty bounds for the maximum horizontal stress using the procedure illustrated in Figure 1.

Finally, we perform a Mohr-Coulomb analysis for the major earthquake locations (as listed in Table 1) within the NMT and KSMMA to explain why the presence of transtensional and transpressional stress regimes favors fault reactivation.

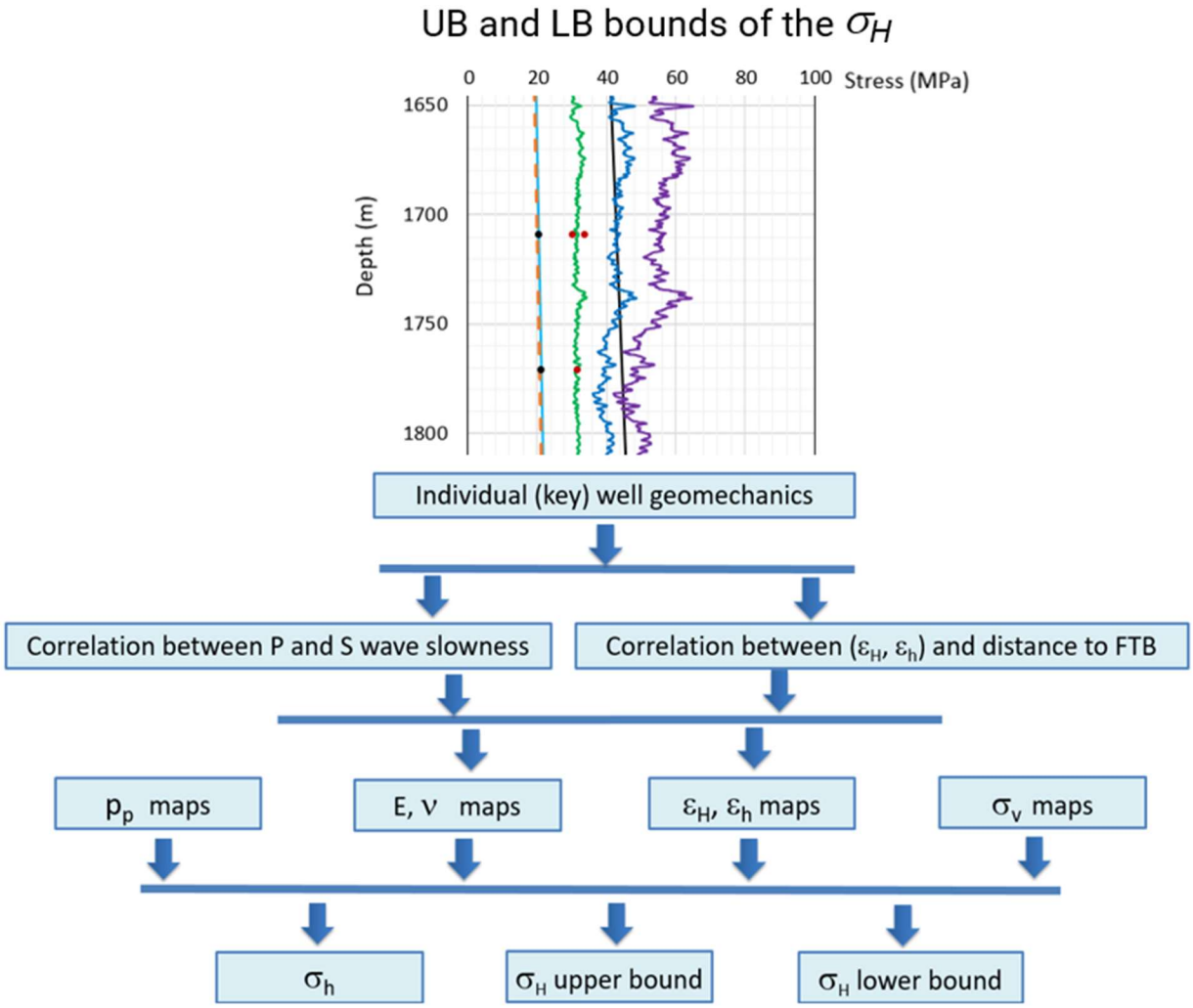

Figure 1 Flowchart for estimating areal in-situ stress magnitudes. Curves on the top are examples from a key well and are calibrated using formation pore pressure measurement data and DFIT closure pressure. Cyan: pore pressure, dashed orange: equivalent circulation density of drilling mud, green: minimum horizontal stress, black: vertical stress, blue: lower bound of the maximum horizontal stress, purple: upper bound of the maximum horizontal stress. Synthetic shear wave sonic slowness logs are generated for wells with only compressive sonic slowness data. The relationship between horizontal strain corrections and the distances to the FTB are correlated from the key wells.

Observations

It is observed that a reverse faulting to transpressional stress state exists within the NMT area, transitioning to a transtensional to normal faulting regime in the East of KSMMA (as shown in Figure 2).

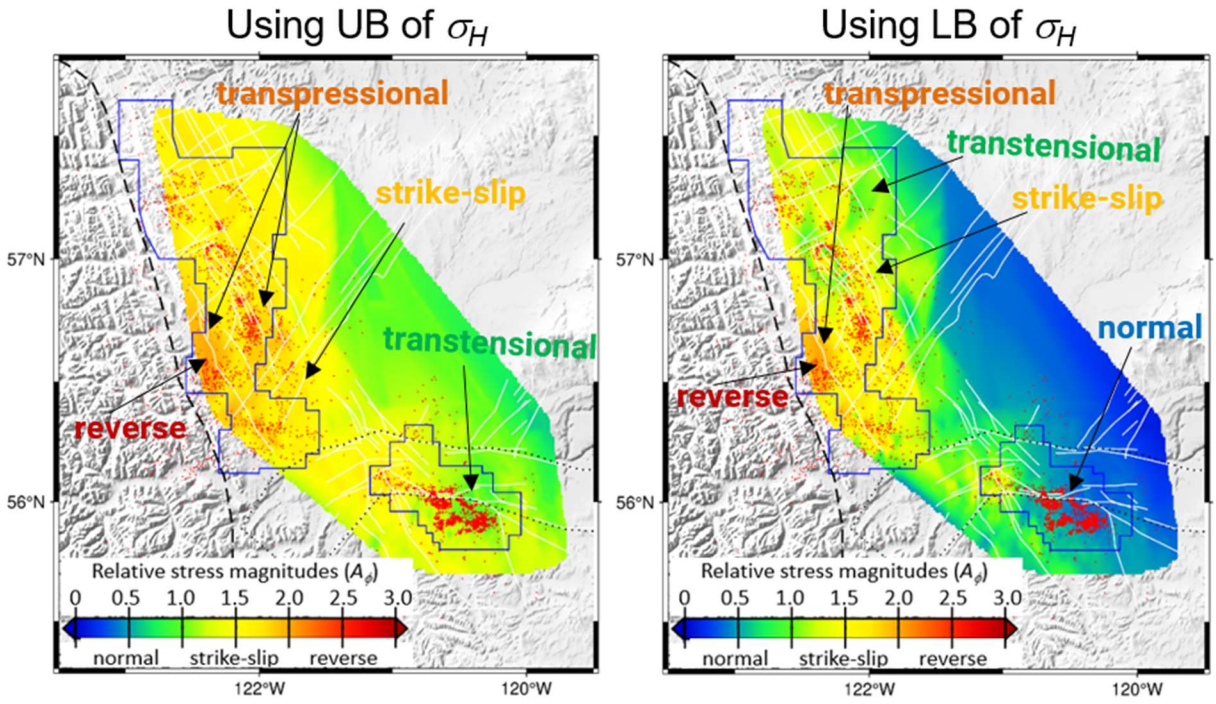

Figure 2 Anderson fault parameter A_ϕ calculated for the commingled Montney Formation using the upper (left) and lower (right) bounds of the maximum horizontal stress. Red dots are the recorded seismicity locations (magnitude of 1.5 or higher) from 2000 to 2023 (British Columbia Energy Regulator, 2024). White lines are faults. The black dashed line stands for the outcrop edge of the Rocky Mountain FTB. The black dotted polygon indicates the FSJG. The NMT and KSMMA areas are shown as blue polygons.

We also found that the recorded seismicity mainly occurred close to transitional in-situ stress regime locations, as in these cases fault reactivation can occur on multiple planes, including both strike-slip and normal (KSMMA), or strike-slip and reverse (NMT) faults.

Mohr-Coulomb failure analyses based on the estimated stresses show that the M_W=4.6 event in the NMT is caused by a thrust-faulting reactivation of a NW-SE oriented low dip angle fault; the other three events (M_L=3.6~4.3) near the southern margin of the FSJG are caused by a strike-slip reactivation of some high-dip angle listric faults.

Conclusions

We estimated full in-situ stress tensors for the Montney Formation, British Columbia. From West to East, the stresses transition from reverse to transpressional to strike-slip in the Northern Montney trend, and from strike-slip to transtensional/normal faulting in the Kiskatinaw Seismic Monitoring and Mitigation Area.

In the study area, seismicity does not necessarily occur in areas with the highest pore pressures, but is located predominantly in transitional stress regimes, where two principal stresses have similar magnitudes because here more than one set of optimal fault orientations exists for reactivation.

Mohr-Coulomb failure analyses based on the estimated stresses show that resulting fault slip potentials are in agreement with focal mechanism observations for three out of four moderate-sized events in the Montney Formation, providing further evidence that the estimated stresses and their bounds are representative.

Acknowledgments

The authors thank the sponsors of the Consortium of Distributed and Passive Sensing (C-DaPS) for financial support. Thanks to (i) GeoLOGIC systems ltd. for their contribution of data and software used in this study; (ii) Enlighten Geoscience Ltd. for providing pore pressure and DFIT data from their previous study; and (iii) an anonymous company for providing logging data, core test data, and DFIT data. The authors are also grateful to (i) BCER for the permission to access the online library, (ii) R. Pradisti who generated the induced seismicity catalog based on data provided by the Geological Survey of Canada, (iii) A. Yaghoubi and J. Parra who shared the shape files, (iv) D. Eaton who shared the list of suggested focal mechanism results of the Montney Formation, and (v) X. Yang and W. Fadil who helped with the mapping process.

References

British Columbia Energy Regulator. (2024). British Columbia's Induced Seismicity Catalogue. https://www.bcogc.ca/files / operations - documentation / Induced - Seismicity - Data-and-Submission/main origin mag 1point5ml up.csv.

Eaton, D. W., & Schultz, R. (2018). Increased likelihood of induced seismicity in highly overpressured shale formations. Geophysical Journal International, 214 (1), 751–757.

Hamidbeygi, M., Vasyura-Bathke, H., Dettmer, J., Eaton, D. W., & Dosso, S. E. (2023). Bayesian estimation of non-linear centroid moment tensors using multiple seismic data sets. Geophysical Journal International, 235(3), 2948–2961.

Han, H., & van der Baan, M. (2024). Constraint strategies for estimating in-situ stress from borehole measurements. Geomechanics for Energy and the Environment, 37, 100518.

Mahani, A. B., Schultz, R., Kao, H., Walker, D., Johnson, J., & Salas, C. (2017). Fluid injection and seismic activity in the northern Montney play, British Columbia, Canada, with special reference to the 17 August 2015 Mw 4.6 induced earthquake. Bulletin of the Seismological Society of America, 107(2), 542–552.

Salvage, R. O., & Eaton, D. W. (2022). The influence of a transitional stress regime on the source characteristics of induced seismicity and fault activation: Evidence from the 30 November 2018 Fort St. John ML4.5 induced earthquake sequence. Bulletin of the Seismological Society of America, 112(3), 1336–1355.